THE PUBLISHING HOUSE
OF THE ROMANIAN ACADEMY

PROCEEDINGS OF THE ROMANIAN ACADEMY, Series A,
Volume 24, Number 4/2023, pp. 339–348
DOI: 10.59277/PRA-SER.A.24.4.06

RESEARCH OF THE WIFI/WIMAX PATCH TYPE ANTENNA ON VARYING EMBEDDED MATERIAL'S DIMENSIONS

Darius PLONIS, Raimondas POMARNACKI, Diana BELOVA-PLONIENĖ, Andrius KATKEVIČIUS, Vaiva RUSEN

Vilnius Gediminas Technical University, Department of Electronic Systems, Plytinės str. 25, LT-10105, Vilnius, Lithuania
Corresponding author: Darius PLONIS, E-mail: darius.plonis@vilniustech.lt

Abstract. The microstrip patch antenna with the feeder gap is improved with nematic liquid crystal of type E7 embedded material, which has replaced the part of dielectric substrate. The investigation is focused on the impact of the geometrical parameters of the fragment of embedded material to the *S* parameters of the microstrip patch antenna. Authors presents initial simulation results to investigate how embedded material influences and changes typical antenna electrical characteristics. The computer-based modeling is performed with Ansys HFSS®. The embedded material has allowed to control the resonance frequencies and directivity and also to improve the gain of the antenna. The best case is obtained with –21.76 dB return loss at 2.4 GHz frequency when the length and width of the fragment of embedded material were equal to 1 mm and 20 mm respectfully. The designed antenna is characterized by good directivity when all energy is concentrated in main lobe.

***Key words**:* microstrip patch antenna, embedded material, resonance frequency.

1. INTRODUCTION

Different constructions and materials of microstrip patch antennas are already investigated in details [1–3]. Microstrip patch antennas are adapted to work for specific applications in a variety of different frequencies [4, 5]. Such a large variety is required because of the WiMAX standard, which could work in the frequency range from 2 GHz till 11 GHz. The working distance is till 10 kilometers. The WiMAX standard has variety of channel bandwidths [6, 7]. Microstrip patch antennas are also connected and used in antenna arrays [8]. Although these antennas are widely studied, there are still many areas for research.

One of the areas is the investigation of the new materials which could be used as the base of the antenna. Scientist are looking for the new materials in order to extract new electrical properties of the antennas, such as a higher center frequency, wideband, multiple center resonances and special directivity properties [9, 10]. The new materials also allow to make tunable microstrip patch antennas [11].

For example, the authors in [12] developed an antenna which operates at 60 GHz frequency with a gain of 7.91 dB. 5 different base materials which were found in the Ansys HFSS® antenna modeling tool were used in the study. Other works [13–19] also investigated the different materials and structures of antennas. These structures usually have the rectangular shape. Among the more interesting studies is the design of antennas on portable materials or clothes [20]. Authors have used textiles and leather products and made the computer-based modeling in order to investigate the performance of such antennas.

Special attention is currently being paid to metamaterials. For example, the authors in [21] have inserted periodically the miniature spheres of metamaterial into the framework of antenna. As a result, the flexible base of the antenna was obtained and the electrical properties of the antenna were improved. On the other hand, the production of such a base is complicated. The authors in [22] have covered the surface of the FR4 base with a thin layer of Yttrium-iron and have formed a silver microstrip antenna on it [22]. As a result, the return loss of the antenna was equal to –19.67 dB, the resonant frequency was equal to about 6.42 GHz and the bandwidth was equal to 3.13 GHz. The identical embedded material was also used in [23]. Authors claim that the embedded material allowed to increase the bandwidth area by at least 70 %. Similar results were obtained in [24].

The construction of the microstrip patch antenna was also improved by using the metamaterials. Authors claim that the bandwidth was increased from hundreds of MHz till GHz.

One of the most important features of the microstrip patch antennas with metamaterials is that these antennas can be controlled by electric or magnetic fields. This feature allows to change the properties of the antenna in real time. For example, authors in [25, 26] have placed the small layer of ferrite under the antenna conductor. The incorporation of ferrite allowed the authors to linearly control the resonance frequency [26]. In addition, it has been observed that the antenna operates in a circular polarization manner. The authors have mentioned that this action is completely different than using a ferrite material for the whole base.

In order to protect the antenna from external influences, an additional layer of material can be placed on top of the antenna [27]. The authors have placed the superstrate on top of the antenna. This modification has allowed to reduce the size of the antenna by 30 %. The materials and the cylindrical shape of the antenna have allowed to obtain the triple band antenna. However, these modifications have also reduced the center frequencies of the antenna. The thicker the superstrate, the lower the frequencies. This is due to the fact that the upper dielectric acts on the lower frequency. As a result, the electromagnetic fields are changed.

It is also possible to add some complex structured materials inclusions as shown in [28]. According to the authors, the main advantage is that the center frequency has risen and the size of the device has decreased. This is in line with the observations of other authors' articles.

The next three examples discuss and show the advantages of patch antennas with liquid crystals in antenna design. The design and optimization of a dual-band microstrip patch antenna using Nematic 5CB liquid crystal on a glass substrate having relative permittivity of 6.438 is presented in [29]. The 5CB nematic liquid crystal has filled the 0.005 mm gap between to glass substrate of 21×25 mm^2 and 19×19 mm^2 dimensions. According to the authors, the proposed antenna operates in dual bands, resonating at 1.8 GHz and 9.2 GHz, with improved characteristics such as S_{11} of –27 dB and –19.42 dB respectively. As an advantages, the band width and reflection coefficients are highlighted.

Authors from [30] have proposed the tunable THz 1-D leaky-wave antennas based on nematic liquid crystals. Authors claim that the key advantage was the tunability of the antenna. Nematic Liquid Crystals exhibit tunable electrical properties under an applied electric field, allowing for dynamic control of the antenna characteristics. The proposed antenna has also allowed to cover a wider range of terahertz frequencies. As additional features the low-loss characteristics and compact design were mentioned.

Similar advantages are mentioned in [31]. The microstrip patch antenna with nematic liquid crystal (N-LC) cell which serves as substrate, has allowed to alter the resonant frequency of the antenna with relatively low applied external voltages. Authors achieved frequency tuning range between 5.45 GHz and 5.84 GHz with return loss higher than 20 dB. The tuning frequency range was achieved with a low voltage between 0 and 5 V.

The model of the typical 2.4 GHz microstrip patch antenna with embedded material which replaces the part of dielectric substrate is presented in this paper. The aim of this work is to investigate the properties of such antenna and to present the initial simulation results about the influence of sizes of embedded material to the central frequencies, gain, directivity of the presented antenna.

2. ELECTRODYNAMICAL MODEL OF PATCH ANTENNA WITH EMBEDDED MATERIAL

The influence of embedded material to the operation of microstrip patch antennas is investigated using the conventional model of microstrip patch antenna with an input feeder gap (Fig. 1).

The conventional model of microstrip patch antenna without an embedded material is chosen to operate at the 2.4 GHz central frequency. The conventional model of microstrip patch antenna is chosen for the analysis because this type of antenna is already investigated in details and the results of this type of antenna could be considered as a reference for our investigation. The results of antenna with embedded material will be properly and objectively compared with results of conventional microstrip patch antenna without embedded material.

The resonant frequency of the antenna should be equal to 2.4 GHz. The FR4 material with $\varepsilon_r = 4.3$ is selected for the dielectric substrate. The selected thickness of the substrate h is equal to 1.6 mm and the thickness of conductor t is equal to 0.035 mm (1 oz). These parameters were selected according to possible materials and parameters in the manufacture.

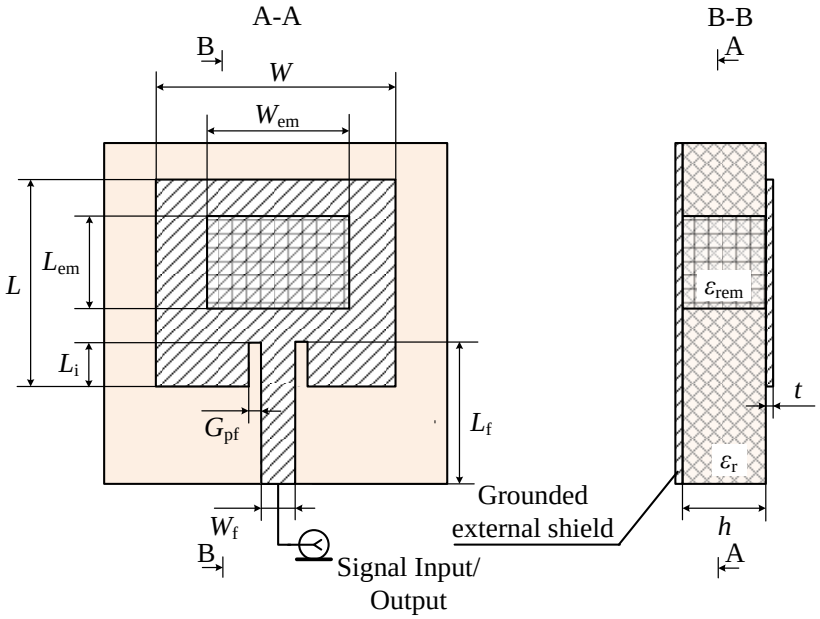

Fig. 1 – The conventional microstrip patch antenna with a feeder gap and the specified possible position of the embedded material where W is the width of the patch, L is the length of the patch, h is the thickness of dielectric substrate, t is the thickness of the conductor; W_f is the width of feeder, L_f is the length of feeder, G_{pf} is the gap between the patch conductor and the feeder, L_i is the length inset of the patch for the feeder line, L_{em} is the length of possible embedded material, W_{em} is the width of possible embedded material, ε_r is the permittivity of the dielectric substrate, ε_{rem} is the permittivity of the embedded material.

Other design parameters of the microstrip patch antenna with feeder gap are calculated by equations (1)–(8). The width W of the patch antenna is calculated by using (1) equation.

$$W = \frac{c}{2 f_0 \sqrt{\frac{\varepsilon_r + 1}{2}}}, \tag{1}$$

where W is the width of patch antenna, c is the speed of light in vacuum 3×10^8 m/s, f_0 is the resonant frequency, ε_r is the dielectric substrate with permittivity equal to 4.3.

The effective dielectric permeability is calculated by using the (2) equation

$$\varepsilon_{reff} = \frac{\varepsilon_r + 1}{2} + \frac{\varepsilon_r - 1}{2}\left(1 + 12\frac{h}{W}\right)^{-1/2}, \tag{2}$$

where ε_{reff} is the effective dielectric permeability and h is the thickness of dielectric substrate.

Effective length of the microstrip patch antenna L_{eff} is calculated from already known parameters

$$L_{eff} = \frac{c}{2 f_0 \sqrt{\varepsilon_{reff}}}. \tag{3}$$

Fringing length ΔL is calculated by using (4) equation

$$\Delta L = 0.412h\frac{\left(\varepsilon_{reff} + 0.3\right)\left(\frac{W}{h} + 0.264\right)}{\left(\varepsilon_{reff} - 0.258\right)\left(\frac{W}{h} - 0.8\right)}. \tag{4}$$

Final length L is calculated by using (5) equation

$$L = L_{eff} - 2\Delta L. \tag{5}$$

The length and width of the earth's surface L_g and W_g are calculated using (6) equations

$$L_g = 2L\,,\quad W_g = 2W\,. \tag{6}$$

Typically, the input characteristic impedance Z_c is 50 Ω. The gap area G_{pf} between the patch conductor and the feeder is typically 1 mm and the width of the feeder W_f is estimated approximately in order to satisfy the predicted value of the characteristic impedance

$$Z_c = \begin{cases} \dfrac{60}{\sqrt{\varepsilon_{reff}}}\ln\left(\dfrac{8h}{W_f}+\dfrac{W_f}{4h}\right), & \dfrac{W_f}{h}\le 1 \\ \sqrt{\varepsilon_{reff}}\left[\dfrac{W_f}{h}+1.393+0.667\ln\left(\dfrac{W_f}{h}+1.444\right)\right], & \dfrac{W_f}{h}\ge 1, \end{cases} \tag{7}$$

where the inset depth of the feeder L_i is calculated by using (8) equation

$$L_i = 10^{-4}\begin{pmatrix} 0,001699\varepsilon_r^7 + 0,13761\varepsilon_r^6 - 6.1783\varepsilon_r^5 + \\ +93.187\varepsilon_r^4 - 682.69\varepsilon_r^3 + 561.9\varepsilon_r^2 - \\ -4043\varepsilon_r + 6697 \end{pmatrix}\frac{L}{2}\,. \tag{8}$$

Based on the (1)–(8) equations, the microstrip patch antenna with feeder gap and working at 2.4 GHz central frequency should have the following design parameters: the width $W = 38$ mm, the length $L = 29$ mm; the length inset of the patch for the feeder line $L_i = 8.85$ mm; the distance between the patch conductor and the feeder $G_{pf} = 1$ mm and the width of the feeder conductor $W_f = 3.137$ mm. These parameters are obtained with the FR4 dielectric substrate which parameters are $\varepsilon_r = 4.3$ and $h = 1.6$ mm. The copper conductor is used in modelling, which thickness $t = 0.035$ mm and conductivity is equal to 5.8×10^7 S/m.

The directivity of an antenna in a given direction is the ratio of the radiation intensity in a given direction from the antenna to the radiation intensity averaged over all directions by the IEEE Standard for Definitions of Terms for Antennas [32]. The average radiation intensity is equal to the total power radiated by the antenna divided by 4π. If the direction is not specified, the direction of maximum radiation intensity could be implied. For the analysis of antenna could be used term directive gain and basically it is the same as directivity.

The calculated design parameters are used in computer-based modelling procedure. The computer-based modeling is done by using the Ansys HFSS® commercial software package. The calculated characteristics of the conventional microstrip patch antenna with feeder gap are presented in Fig. 2. According to the results, the conventional microstrip patch antenna has good resonance properties at 2.4 GHz frequency. The return loss S_{11} characteristic reach –18 dB (Fig. 2a). The resonance frequencies occur also repeatedly in higher frequencies. The results are presented in the range from 0 till 5 GHz.

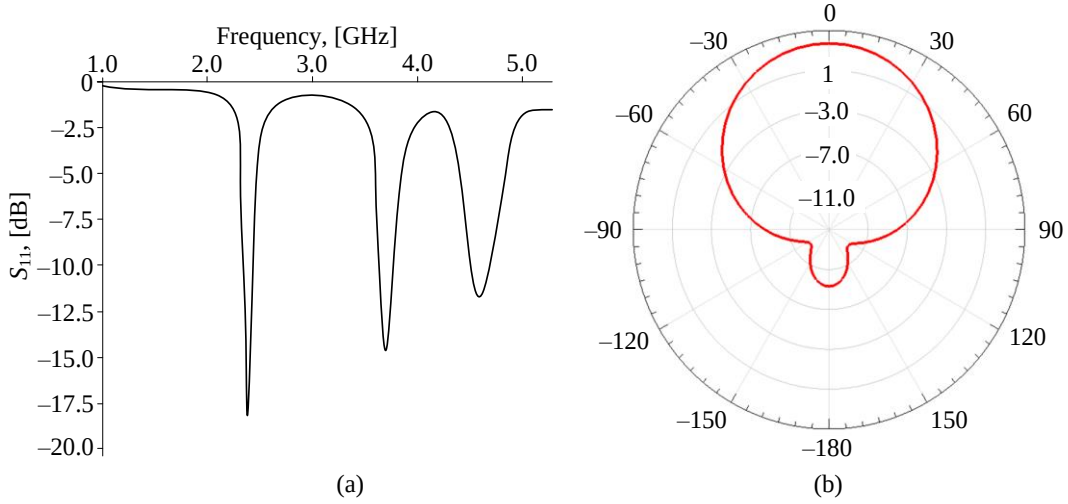

Fig 2 – The return loss S_{11} (a) and directivity (b) characteristics of the microstrip patch antenna with feeder gap.

The calculated directivity characteristic perfectly corresponds to the practical and theoretical modeling characteristics (Fig. 2b). The antenna is directional and here are no side lobs at all.

This model of conventional antenna and its results will be considered as a reference for the comparison purpose with the model of our presented microstrip patch antenna with the feeder gap which is supplemented by the embedded material. The position of the embedded material in the overall geometry of the microstrip patch antenna with the feeder gap is presented in Fig. 1.

The width W_{em} and length L_{em} of the embedded material will vary during the experiment. The W_{em} and L_{em} do not exceed over the conductor edges of patch antenna. The thickness of the embedded material will be the same as the FR4 material and equal to 1.6 mm. The nematic liquid crystal of type E7 from Merck Laboratories embedded material will be used in the experiment. The permittivity of such material could be changed by changing the DC voltage usually from 0 to 10 V and the dielectric constant should vary by 30 %. At low voltage input (millivolts range) relative dielectric permittivity equal to $\varepsilon_{rem} = 2.72$. The comparison and analysis of results are presented in next Section.

3. RESULTS

The results section is divided into the formal analysis of the microstrip patch antenna and comparison of the microstrip patch antenna with other research's results subsections.

3.1. Formal analysis of the microstrip patch antenna

Experimental analysis of a microstrip patch antenna with an embedded specialized material was performed using Ansys HFSS® commercial software package.

The width W_{em} of the embedded material has varied in the range from 1 mm till 38 mm. The length L_{em} of the embedded material has varied in the range from 1 mm till 29 mm. The width and length of the embedded material were increased by 1 mm at each step of analysis. 1102 iterations of analysis experiments were performed in all and it lasted a couple of weeks using a PC with an Intel Core I5-7600 microprocessor and 8 GB of RAM. About 168 GB of data were generated during the experiment.

The analysis is performed from 0 till 10 GHz frequency range with the step size of 0.1 GHz. The results are given from 0 up to 5 GHz, as no practically useful results have been observed at higher frequencies. Several frequency points were selected for the deeper analysis from the 0–5 GHz frequency range as a strong radiation effect was observed at these frequencies during the plenary experiment (Fig. 3) and (Fig. 4).

The dependency of resonant frequency on the variation of the width W_{em} of embedded material are presented in (Fig. 3). The length L_{em} of the embedded material is constant and equal to 3 mm.

The analysis of the reflection coefficient S_{11} has shown that the resonant frequency can be slightly shifted to the higher or lower frequencies when the width W_{em} of the embedded material is changed. It should be emphasized, that the dependency of resonant frequency on the W_{em} is not linear. For example, the resonance frequency increases from 2.4 GHz to 2.5 GHz when the width is increased from 18 mm till 19 mm. The resonance frequency is equal to 2.4 GHz again when $W_{em} = 20$ mm. The resonance frequency shifts to higher frequencies by 200 MHz and is equal to 4.7 GHz when W_{em} increases from 18 mm till 19 mm. The resonance frequency is even smaller and equal to 4.4 GHz when $W_{em} = 20$ mm.

The dependency of resonant frequency on the variation of the width W_{em} and length L_{em} of embedded material are presented in (Fig. 4). Only a small part of the experimental results that showed better resonance properties with S_{11} equal or less than –20 dB at certain frequencies are presented.

According to the results, good resonant properties at 2.4 GHz frequency are obtained when L_{em} is not greater than 2 mm and W_{em} is not greater than 20 mm. In all other cases, the S_{11} is above –10 dB. The overall width W of the patch of antenna is equal to 38 mm.

It is also necessary to mention that the insertion of the embedded material not only allows to vary the resonance frequency but also improves the return loss S_{11} characteristics. The best case with –21.76 dB return loss at 2.4 GHz frequency is obtained when the length L_{em} of inserted embedded material is equal to 1 mm and the width W_{em} is equal to 20 mm. For example, a microstrip antenna of the same dimensions but without the embedded material gives only –18.04 dB return loss. Similar improved results of S_{11} are obtained and near other resonance frequencies.

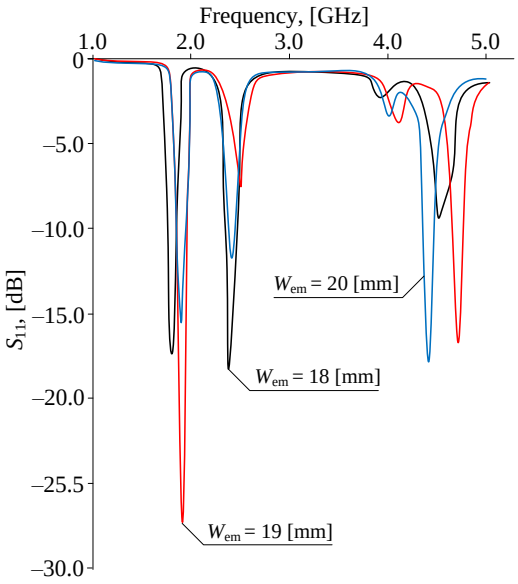

Fig. 3 – Dependency of resonant frequencies on the variation of width W_{em} of the embedded material when the length L_{em} is constant and equal to 3 mm.

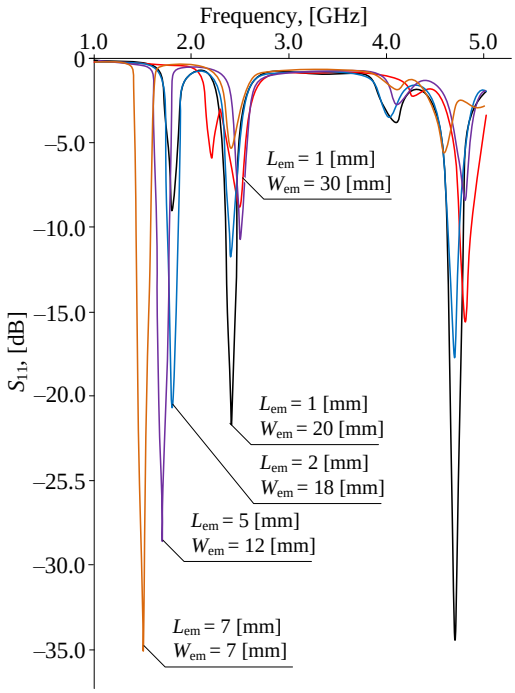

Fig. 4 – Dependency of resonant frequencies on the variation of the length L_{em} and width W_{em} of the embedded specialized material.

In a broader analysis and without focusing only on the 2.4 GHz frequency it can be observed that the combination of $L_{em} = 1$ mm and $W_{em} = 20$ mm dimensions of the embedded material gives good resonance properties also at 4.7 GHz frequency. The S_{11} is equal to –34.89 dB. It is also necessary to note that additional resonance frequencies occur between 1.5 GHz and 2.1 GHz frequencies when the length L_{em} of the embedded material increases. For example, the $S_{11} = -35$ dB resonance occurs at 1.5 GHz frequency when $L_{em} = 7$ mm and $W_{em} = 7$ mm.

Moreover, when the length L_{em} of the embedded material increases by more than 7 mm, the radiation properties of the antenna degrade. This effect could be caused by the electrical field distribution. These 7 mm are already ~ 1/4 of the overall length L of the antenna. Therefore, the electrical field of embedded material is more effected by the feed and the gap of antenna.

The directional diagram and radiation pattern are other important characteristics that were taken into account. We have selected to discuss the cases when the directional diagram is approximately symmetrical. All other results with other combination of L_{em} and W_{em} parameters simply repeat the same results or are worse in comparison with presented results.

The designed antenna is directional at 2.4 GHz frequency when $L_{em} = 1$ mm and $W_{em} = 20$ mm (Fig. 5a). Almost all energy is concentrated in main lobe. The return loss is equal to –21.76 dB. There is also a very small back lobe and no side lobs. The directivity of the main lobe is equal to about 90°. The radiation pattern shows that the orientation of the main lob of the microstrip patch antenna with feeder gap and embedded material is directed towards the top of the antenna (Fig. 5b).

Although the antenna was not designed for 4.7 GHz frequency, there is a very high return loss $S_{11} = -34.89$ dB at 4.7 GHz when $L_{em} = 1$ mm and $W_{em} = 20$ mm. This time the directional diagram shows that antenna is bidirectional. Both lobes have similar amount of energy but lobes are not symmetrical (Fig. 6a). The radiation pattern shows that the directivity is more lateral than to the top of the antenna (Fig. 6b). This is a useful feature when the antenna is properly positioned in the space.

As it was mentioned before, resonances occur also at lower frequency range when the length L_{em} of the embedded material increases. The return loss of –35.08 dB is obtained at 1.5 GHz with $L_{em} = 7$ mm and $W_{em} = 7$ mm. This time the directional diagram has two side lobes which are fully symmetrical (Fig. 7a).

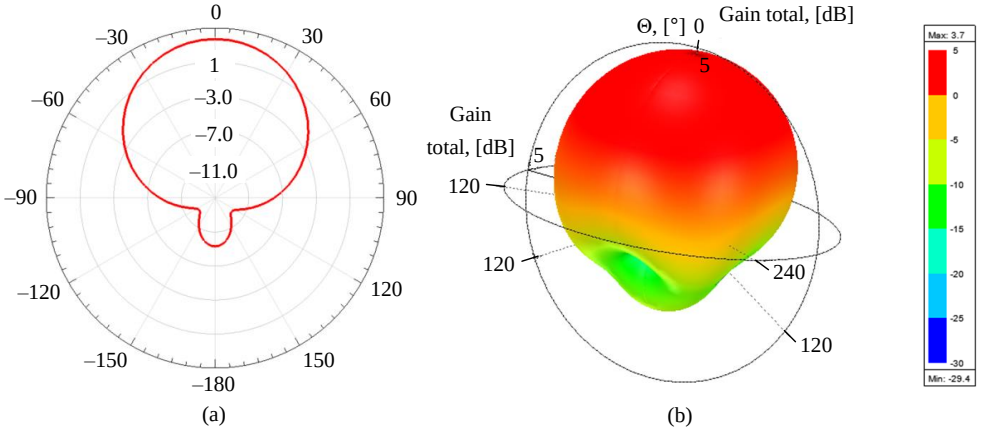

Fig. 5 – The directivity diagram (a) and 3D radiation pattern (b) of the microstrip patch antenna with an input feeder gap when the length and width of the embedded material are L_{em} = 1 mm and W_{em} = 20 mm and frequency is equal to 2.4 GHz.

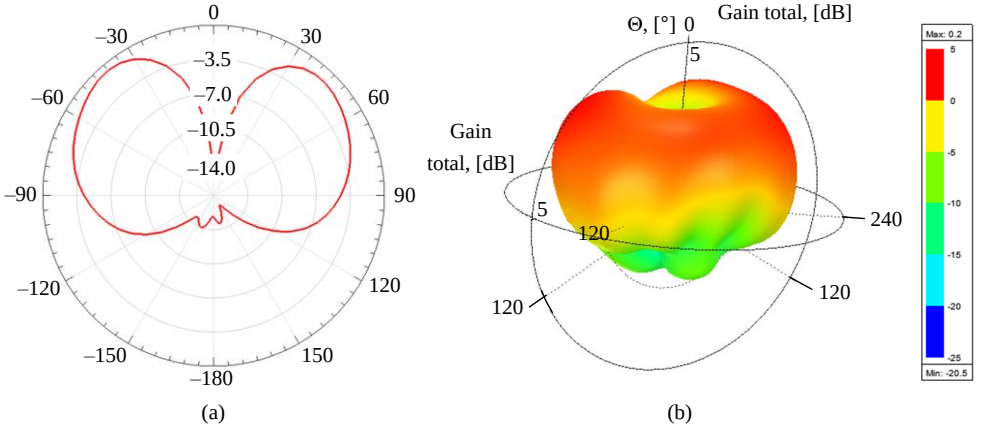

Fig. 6 – The directivity diagram (a) and 3D radiation pattern (b) of the microstrip patch antenna with an input feeder gap when the length and width of the embedded material are L_{em} = 1 mm and W_{em} = 20 mm mm and frequency is equal to 4.7 GHz.

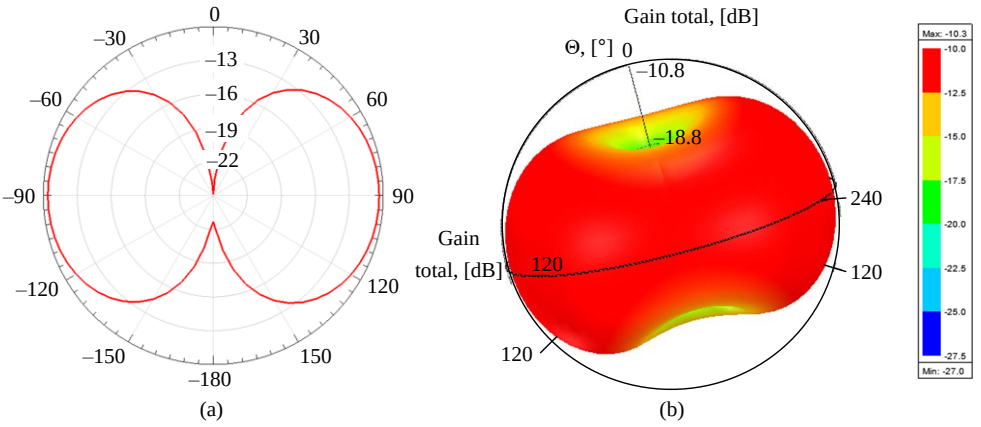

Fig. 7 – The directivity diagram (a) and 3D radiation pattern (b) of the microstrip patch antenna with an input feeder gap when the length and width of the embedded material are L_{em} = 7 mm and W_{em} = 7 mm and frequency is equal to 1.5 GHz.

It could be seen from the radiation pattern that in this case the directivity is completely lateral to the sides (Fig. 7b).

3.2. Comparison of the microstrip patch antenna

Resonance frequency and bandwidth parameters of the microstrip patch antennas with embedded materials were selected for the results comparison with other research. In addition, two new materials were selected for the substrate of the microstrip patch antenna ($L_{em} = 3$ mm and $W_{em} = 19$ mm) in order to analyze the return loss S_{11} characteristics of the designed antenna. The permittivity is equal to $\varepsilon_r = 3.8$ and dielectric loss factor is less than 0.0004 of the first Fused Quartz (FQ) material. The second Silicon (Si) material is loss free and its permittivity is equal to $\varepsilon_r = 11.7$.

First of all, it could be seen from the dependencies of the bandwidth on the resonance frequency, that bandwidth varies from 150 MHz to 250 MHz and resonance frequencies varies from 2.5 GHz to 2.7 GHz, when the substrate of the microstrip patch antennas is made from FR4, FQ, Si respectively. It means, that the higher resonance frequency could be obtained with FQ substrate of the designed antenna. The narrowest bandwidth 150 MHz of designed antenna could be received in case when loss free Si substrate is used. However, more resonances could be noticed from the return loss S_{11} characteristics. These resonances could influence the operation of the microstrip patch antenna. On the other hand, bandwidth of 150 MHz is sufficient for the WiFi technologies (Fig. 8).

It could be seen from the comparison results with other researchers' works (see Fig. 8), that the proposed antennas could operate in higher frequencies [31] in case the nematic liquid crystal (N-LC) cell has been used. The resonance frequency of the proposed antenna is 4.76 GHz, when external bias voltage is 0. Furthermore, the resonance frequency of the 6CB nematic liquid crystal (6CB NLC) based rectangular patch antenna for S-band and C-band applications moves to lower frequencies and is equal to 3.3 GHz. The bandwidth of the proposed antenna with 6CB NLC in simulation case is equal to 1.84 GHz (see Fig. 8).

The resonance frequency could be observed at 1.8 GHz frequency, when Moth Flame Optimization (MFO) algorithm is used, in the case of the nematic 5CB liquid crystal based dual band microstrip patch antenna [29]. However, in this case the widest bandwidth of liquid crystal based dual band microstrip patch antenna could be received and it is equal to 2.15 GHz (Fig. 8).

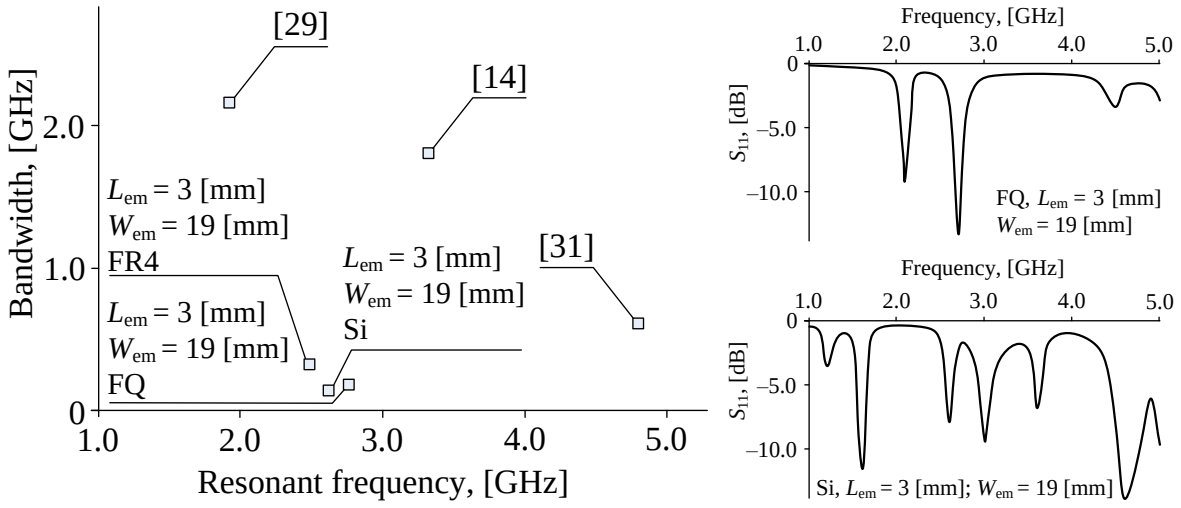

Fig. 8 – The comparison of the analysis results of the bandwidth and resonant frequencies of the microstrip patch antennas with embedded materials.

Summarizing, the obtained results well correlated with the results discussed in the scientific literature during the qualitative comparison – improved gain, wider and adjustable operating frequency range. Only in our analysis case we have a very narrow bandwidth. Therefore, our proposed antenna is more selective. Moreover, the analysis has shown that the substrates from the higher dielectric permittivity will change the bandwidth. Likewise, the bandwidth of the microstrip patch antennas with nematic liquid crystals embedded materials will be narrower.

4. DISCUSSION

The designed microstrip patch antenna with an additional section of embedded material has shown positive features. The presented antenna could be used in communication networks of IoT devices working at 2.4 GHz central frequency. The variation of dimensions of inserted embedded material provides the additional ability to slightly shift the resonance frequency of the designed antenna. This allows freedom in the configuration of the IoT transmission systems. It is also important that the inserted embedded material improves the return loss S_{11} characteristics of the designed antenna. This allows to reduce signal reflection, improve enhanced matching between antenna and transmission line, increase signal efficiency. A well-matched antenna with low return loss is more stable and reliable in various operating conditions, leading to consistent performance.

The obtained positive features encourage the continuation of work in this direction and, in addition, to induce embedded material with the different electrical field and compare results while antenna is controlled in the "passive mode". Another future direction could be the miniaturization of the antenna. Shifting the antenna's resonance frequency to higher frequencies due to the insertion of the embedded materials presupposes the possibility of miniaturizing the antenna while maintaining the current characteristics of the antenna.

The proposed antenna with embedded materials also poses additional challenges. The biggest challenge will be the increase of the number of steps in the manufacture of the presented antenna. Additional steps of etching, cutting, embedding, crystal production will require separate orders and increase production costs.

5. CONCLUSIONS

The specialized embedded material was included into the dielectric of conventional microstrip patch antenna with feeder gap. The design parameters of the antenna with embedded material were calculated using the standard techniques which are customized for the conventional microstrip patch antenna with feeder gap.

The embedded material which has replaced the part of dielectric substrate has improved the electrical characteristics of the microstrip patch antenna with the feeder gap. For example, the return loss was improved by 3.72 dB from –18.04 dB till –21.76 dB at the most interesting for us 2.4 GHz frequency. The improved results were also obtained at others resonance frequencies.

The variation of length and width of embedded material allows to slightly shift the resonance frequency to lower or higher frequencies without changing the overall dimensions of the microstrip patch antenna.

The change of directivity diagram has been observed when the length of embedded material has increased. The antenna has changed from directional with one main lobe into the bidirectional with two symmetrical lobes.

REFERENCES

1. V. PRAKASAM, N. REDDY, *Hexagonal shaped micro-strip patch antenna design for 2.45 GHz WLAN system*, 6th International Conference on Inventive Computation Technologies (ICICT), Coimbatore, India, 2021, pp. 13–18.
2. A.S.A. GAID, S.M.E. SALEH, A.H.M. QAHTAN, S.G.A. AQLAN, B.A.E. YOUSEF, A.A.A. SAEED, *83 GHz microstrip patch antenna for millimeter wave applications*, International Conference of Technology, Science and Administration (ICTSA), Taiz, Yemen, 2021, pp. 1–4.
3. B. MANOJ, S. RODRIGUEZ, *Genetic algorithm optimization of MicroStrip Patch Antenna dimensions for enhanced bandwidth, accurate operating frequency and return loss*, Sixth International Conference on Wireless Communications, Signal Processing and Networking (WiSPNET), Chennai, India, 2021, pp. 441–445.
4. N. SAKIB, S.N. IBRAHIM, M. IBN IBRAHIMY, M.S. ISLAM, M.M.H. MAHFUZ, *Design of microstrip patch antenna on rubber substrate with DGS for WBAN applications*, IEEE Region 10 Symposium (TENSYMP), Dhaka, Bangladesh, 2020, pp. 1050–1053.
5. R. JYOSTHNA, R.A. SUNNY, A.A. JUGALE, M.R. AHMED, *Microstrip patch antenna design for space Aapplications*, International Conference on Communication and Signal Processing (ICCSP), Chennai, India, 2020, pp. 406–410.
6. PRAHLAD, R.A. KANDAKATLA, M. PRASANNA, A.A. JUGALE, M.R. AHMED, *Microstrip patch slot antenna design for WiMAX and WLAN applications*, 3rd International Conference on Trends in Electronics and Informatics (ICOEI), Tirunelveli, India, 2019, pp. 810–814.
7. A. SOKOL, S.T. IMECI, *T-shaped compact microstrip patch antenna for WiMAX applications*, 28th Signal Processing and Communications Applications Conference (SIU), Gaziantep, Turkey, 2020, pp. 1–5.
8. B. OUADIAA, E. ABDELKEBIR, R. ABDELATI, *Microstrip patch antenna array and its applications: a survey*, IOSR Journal of Electrical and Electronics Engineering (IOSR-JEEE), **15**, *1*. pp. 26–38. 2020.

9. H. KASCHEL, C. AHUMADA, *Design of rectangular microstrip patch antenna for 2.4 GHz applied a WBAN*, IEEE International Conference on Automation/XXIII Congress of the Chilean Association of Automatic Control (ICA-ACCA), Concepcion, Chile, 2018, pp. 1–6.
10. Q. LI, H. LIU, *Research on performance of wearable microstrip antenna based on flexible material*, IEEE 5th Advanced Information Technology, Electronic and Automation Control Conference (IAEAC), Chongqing, China, 2021, pp. 245–248.
11. C. MILIAS, R.B. ANDERSEN, P.I. LAZARIDIS, Z.D. ZAHARIS, B. MUHAMMAD, A. MIHOVSKA, D.D.S. HERMANSEN, *Metamaterial-inspired antennas: a review of the state of the art and future design challenges*, IEEE Access, **9**, *1*, pp. 89846–89865, 2021.
12. D. RAKESH, P.R. KUMAR, H. KHAN, K.Ch. SRI KAVYA, B.T.P. MADHAV, K.P. KUMAR, S.B.D. PRASAD, *Performance evaluation of microstrip square patch antenna on different substrate materials*, Journal of Theoretical and Applied Information Technology, **26**, *2*, pp. 97–106, 2011.
13. B. TÜTÜNCÜ, M. KÖSEM, *Substrate analysis on the design of wide-band antenna for sub-6 GHz 5G communication*, Wireless Pers. Commun., **125**, *1*, pp. 1523–1535, 2022.
14. G. SRILEKHA, P. PARDHASARADHI, B.T.P. MADHAV, R.K.N.R. MANEPALLI, M.C. RAO, *Design and analysis of 6CB nematic liquid crystal-based rectangular patch antenna for S-band and C-band applications*, Zeitschrift für Naturforschung A, **75**, *10*, pp. 863–875, 2020.
15. S.D. MAHAMINE, R.S. PARBAT, S.H. BODAKE, M.P. AHER, *Effects of different substrates on rectangular microstrip patch antenna for S-band*, International Conference on Automatic Control and Dynamic Optimization Techniques (ICACDOT), Pune, India, 2016, pp. 1142–1145.
16. O.A. ILESANMI, Ch.U. NDUJIUBA, *Effects of using different substrates on the performance of an inset-fed rectangular microstrip patch antenna*, International Journal of Networks and Communications. **8**, *37*, pp. 37–41, 2018.
17. N. JAYARENJINI, C. UNNI, *A novel microstrip slotted patch antenna using different dielectric substrates for multiple applications*, International Journal of Applied Engineering Research (IJAER), **13**, *1*, pp. 12591–12596, 2018.
18. B. CHAUHAN, S. VIJAY, S.C. GUPTA, *Comparative analysis of microstrip patch antenna using different substrate and observe effect of changing parameter at 5.4 GHz*, Proceedings of the Conference on Advances in Communication and Control Systems, 2013, pp. 729–733.
19. C. CAMACHO-GOMEZ, R. SANCHEZ-MONTERO, D. MARTÍNEZ-VILLANUEVA, P.-L. LÓPEZ-ESPÍ, S. SALCEDO-SANZ, *Design of a multi-band microstrip textile patch antenna for LTE and 5G services with the CRO-SL ensemble*, Applied Sciences, **10**, *3*, art. 1168, 2020.
20. S. JEYAKUMAR, K. SAKTHIMURUGAN, *Wearable textile antenna for ISM band with different dielectric substrate materials*, International Journal of Electronics Engineering Research, **9**, *8*, pp. 1259–1266, 2017.
21. I. PETER, L. MATEKOVITS, *Materials for electromagnetic purpose: the case of a microstrip patch antenna characteristics improvement by additions of metals as spherical inclusions into the substrate*, Acta Marisiensis Seria Technologica, **17**, *1*, pp. 11–16, 2020.
22. I.H. HASAN, M.N. HAMIDON, I. ISMAIL, R. OSMAN, A. ISMAIL, *Yttrium iron garnet thick film inclusion for enhanced microstrip patch antenna performance*, IEEE Regional Symposium on Micro and Nanoelectronics (RSM), Batu Ferringhi, Malaysia, 2017, pp. 131–134.
23. I.H. HASAN, M.N. HAMIDON, A. ISMAIL, I. ISMAIL, A.S. MEKKI, M.A. MOHD KUSAIMI, S. AZHARI, R. OSMAN, *YIG thick film as substrate overlay for bandwidth enhancement of microstrip patch antenna*, IEEE Access, **6**, pp. 32601–32611, 2018.
24. L.W. LI, Y.N. LI, T.S. YEO, J.R. MOSIG, O.J.F. MARTIN, *A broadband and high-gain metamaterial microstrip antenna*, Applied Physics Letters, **96**, *16*, pp. 164101–164105, 2010.
25. P.J. RAINVILLE, F.J. HARACKIEWICZ, *Magnetic tuning of a microstrip patch antenna fabricated on a ferrite film*, IEEE Microwave and Guided Wave Letters, **2**, *12*, pp. 483–485, 1992.
26. A.A. MAVRIDIS, G.A. KYRIACOU, J.N. SAHALOS, *Printed antennas tuned by transversely magnetized ferrite operating at a novel resonant mode*, PIERS Online, **3**, *8*, pp. 1213–1216, 2007.
27. S.K. GUPTA, A. SHARMA, B.K. KANAUJIA, G.P. PANDEY, *Triple band circular patch microstrip antenna with superstrate*, Wireless Personal Communication, **77**, pp. 395–410, 2014.
28. A. SEMICHAEVSKY, A. AKYURTLU, *Homogenization of metamaterial-loaded substrates and superstrates for antennas*, Progress in Electromagnetics Research, **71**, pp. 129–147, 2007.
29. G. SRILEKHA, P. PARDHASARADHI, G. SRINIVAS, N. PRAVEEN, B.T.P. MADHAV, M.C. RAO, M. VENKATESWARA RAO, *A nematic 5CB liquid crystal based dual band microstrip patch antenna using Moth Flame Optimization*, IOP Publishing, **1055**, *1*, art. 01209, 2021.
30. F. WALTER, D.C. ZOGRAFOPOULOS, F. IMPERATO, P. BURGHIGNOLI, R. BECCHERELLI, A. GALLI, *Analysis and design of tunable THz 1-D leaky-wave antennas based on nematic liquid crystals*, Applied Sciences, **12**, *22*, art. 11770, 2022.
31. M.A. CHRISTOU, N.C. PAPANICOLAOU, A.C. POLYCARPOU, *A nematic liquid crystal tunable patch antenna*, The 8th European Conference on Antennas and Propagation (EuCAP 2014), The Hague, Netherlands, 2014, pp. 1875–1878.
32. IEEE Standard Association, *IEEE standard for definitions of terms for antennas*, EEE Antennas and Propagation Society, p. 50, 2014.

Received January 27, 2023